THE JOURNAL OF BIOLOGICAL CHEMISTRY
Vol. 276, No. 40, Issue of October 5, pp. 37149–37154, 2001
Printed in U.S.A.

Folding and Aggregation Are Selectively Influenced by the Conformational Preferences of the α-Helices of Muscle Acylphosphatase*

Received for publication, June 20, 2001, and in revised form, July 25, 2001
Published, JBC Papers in Press, July 30, 2001, DOI 10.1074/jbc.M105720200

Niccolò Taddei‡, Cristina Capanni‡, Fabrizio Chiti‡§, Massimo Stefani‡, Christopher M. Dobson¶‖, and Giampietro Ramponi‡ ‡‡**

From the ‡Dipartimento di Scienze Biochimiche, Università di Firenze, Viale Morgagni 50, Firenze 50134, Italy and the ¶Oxford Centre for Molecular Sciences, New Chemistry Laboratory, University of Oxford, South Parks Rd., Oxford Ox1 3QT, United Kingdom

The native state of human muscle acylphosphatase (AcP) presents two α-helices. In this study we have investigated folding and aggregation of a number of protein variants having mutations aimed at changing the propensity of these helical regions. Equilibrium and kinetic measurements of folding indicate that only helix-2, spanning residues 55–67, is largely stabilized in the transition state for folding therefore playing a relevant role in this process. On the contrary, the aggregation rate appears to vary only for the variants in which the propensity of the region corresponding to helix-1, spanning residues 22–32, is changed. Mutations that stabilize the first helix slow down the aggregation process while those that destabilize it increase the aggregation rate. AcP variants with the first helix destabilized aggregate with rates increased to different extents depending on whether the introduced mutations also alter the propensity to form β-sheet structure. The fact that the first α-helix is important for aggregation and the second helix is important for folding indicates that these processes are highly specific. This partitioning does not reflect the difference in intrinsic α-helical propensities of the two helices, because helix-1 is the one presenting the highest propensity. Both processes of folding and aggregation do not therefore initiate from regions that have simply secondary structure propensities favorable for such processes. The identification of the regions involved in aggregation and the understanding of the factors that promote such a process are of fundamental importance to elucidate the principles by which proteins have evolved and for successful protein design.

The role played by secondary structure in protein folding has been recently actively discussed (1–3). The rational design of mutations increasing the α-helical propensity of regions that are in α-helical conformation in the native state has been one of the most popular experimental strategies adopted to stabilize the native fold of several proteins (4–7). Such conformational stabilization can be largely determined by an increase of folding rate, when the mutated helix is formed to a considerable extent in the folding transition state (5–7). Formation of local secondary structure to an extent similar to that existing in the transition state has been estimated to contribute to a significant, although small, fraction of the activation free energy required for folding (7). Recent experiments on SH3 domains from *drkN* and spectrin have shown that these β-sheet proteins can be strongly stabilized by single mutations that enhance the propensity of a region of the polypeptide chain to form the native β-turn structure (8, 9).

Protein aggregation is the process from which amyloid formation develops. A number of severe human pathologies are based on extracellular deposition of insoluble protein aggregates known as amyloid fibrils (10, 11). These show a common ultrastructural architecture independent of the protein involved in their formation and feature intermolecular β-sheet structure (12). The aggregation process is today considered as a process acting in competition with the normal folding pathway. This concept has derived from the facts that protein aggregation is a common property of any polypeptide chain and that the process takes place from at least partially unfolded states (11, 13). The native protein and the amyloid aggregates can therefore be seen as originating from a common population of partially unfolded, interconverting molecules. In other words, protein aggregation and protein folding are the two sides of the same coin, and it could be argued that structural factors playing relevant roles in one process are also involved in the other one.

Human muscle acylphosphatase (AcP)[1] is an α/β 98-residue protein that has been shown, depending on experimental conditions, to fold following a two-state mechanism (14) or to aggregate to produce amyloid fibrils structurally similar to those associated with disease (15). Two-state folding of AcP occurs through a transition state structure containing a primitive, not completely stabilized, hydrophobic core and significantly formed elements of secondary structure (16–18). A study on the common-type AcP isoenzyme has shown that the second

* This work was supported in part by grants from the Italian Ministero dell'Università e della Ricerca Scientifica e Tecnologica (PRIN Folding e misfolding delle proteine), from the Italian Consiglio Nazionale delle Ricerche (grant 99.02609.CT04), from the Università di Firenze (Fondi d'Ateneo ex 60%), and from The Fondazione Telethon Italia (453.bi). The Oxford Centre for Molecular Sciences was supported by the Biotechnology and Biological Sciences Research Council, the Engineering and Physical Sciences Research Council, and the Medical Research Council. The costs of publication of this article were defrayed in part by the payment of page charges. This article must therefore be hereby marked "*advertisement*" in accordance with 18 U.S.C. Section 1734 solely to indicate this fact.

§ Supported by the Fondazione Telethon Italia.

‖ Supported by the Wellcome Trust.

** Present address: Dept. of Chemistry, University of Cambridge, Lensfield Rd., Cambridge CB2 1EW, United Kingdom.

‡‡ To whom correspondence should be addressed: Tel.: 39-055-413-765; Fax: 39-055-422-2725; E-mail: ramponi@scibio.unifi.it.

[1] The abbreviations used are: AcP, acylphosphatase; TFE, 2,2,2-trifluoroethanol; ThT, thioflavin T; helix-1 (α+), Y25L/D28E AcP variant; helix-1 (α−/β−), E27N/D28N/R31N AcP variant; helix-1 (α−/β+), E27T/D28T/R31T AcP variant; helix-2 (α+), N59A/S60K/S63E/S66A AcP variant.

α-helix of the protein is completely formed in the transition state whereas the first is only partially structured (7). By means of an experimental approach conceptually similar to the φ value analysis introduced by Alan Fersht (19) for the structural characterization of the transition state of folding at a residue level, the aggregation rate has been investigated for a number of AcP mutants[2]. The main results of this study are that AcP aggregation is a highly ordered process taking place from specific regions of the protein and that these regions are highly distinct from those involved in protein folding (17)[2]. AcP has therefore proven to be a particularly suitable model system to investigate folding and aggregation in parallel. In this report we investigate the role of regions corresponding to the two α-helices of AcP and of their propensity to form α-helical structure in folding and aggregation. This provides an opportunity not just to explore the fundamentals of the two processes of folding and aggregation but also to evaluate whether the two processes can be rationally decoupled by specific mutations, an aspect that has relevance for establishing the principles of successful protein design.

EXPERIMENTAL PROCEDURES

Mutants Production and Purification—All the mutants were produced using the QuikChange site-directed mutagenesis kit from Stratagene. The presence of the desired mutations was confirmed by DNA sequencing. All proteins used in this study have cysteine at position 21 replaced by a serine residue, to eliminate complexities in folding reaction associated with the presence of a free cysteine residue (14). For simplicity the protein displaying the sole C21S mutation is referred to as wild-type AcP throughout the manuscript. Cloning, expression, and purification of wild-type and mutated AcP were performed as described by Taddei *et al.* (20). Protein purity was assessed by SDS-polyacrylamide gel electrophoresis. The enzymatic activity of the AcP mutants was measured by a continuous spectrophotometric method, using benzoylphosphate as a substrate (21). Protein concentration was determined by UV absorption using a ϵ_{280} value of 1.49 ml mg^{-1} cm^{-1}.

Equilibrium Experiments—The equilibrium denaturation of wild-type AcP and of its variants was studied by measuring the intrinsic fluorescence of 25–28 equilibrated samples containing various concentrations of urea, ranging from 0 to 8.1 M, in 50 mM acetate buffer pH 5.5, at 28 °C. Protein concentration in each sample was 0.02 mg/ml. A Shimadzu RF-5000 spectrofluorophotometer with excitation and emission wavelengths of 280 and 335 nm, respectively, was used. Each curve, representing the change of fluorescence as a function of urea concentration, was analyzed according to the method of Santoro and Bolen (22) to yield the free energy of unfolding in the absence of denaturants (ΔG^{H_2O}), the dependence of ΔG on denaturant concentration (m value) and the urea concentration at which half of the protein molecules are denatured (C_m).

Kinetic Analysis—Unfolding and refolding reactions were followed using a Shimadzu RF-5000 spectrofluorophotometer with excitation and emission wavelengths of 280 and 335 nm, respectively. All the experiments were performed at 28 °C in 50 mM acetate buffer, pH 5.5, at a final protein concentration of 0.02 mg/ml. The refolding experiments were carried out by a 20-fold dilution of AcP samples denatured in 6 M urea, into solutions containing various concentrations of urea, ranging from 0 to 4.5 M. The unfolding experiments were performed similarly by a 20-fold dilution of urea-free AcP samples into solutions containing urea at concentrations ranging from 3.5 to 8.5 M. The fluorescence traces were fitted to exponential functions to determine the folding and unfolding rate constants k_f and k_u, respectively. Plots of $\ln k_f$ and $\ln k_u$ against urea concentration were fitted to the equation reported by Jackson and Fersht (23) to obtain the natural logarithm of the folding and unfolding rates in water ($\ln k_f^{H_2O}$ and $\ln k_u^{H_2O}$) and their dependences on denaturant concentration (m_f and m_u). The m, ΔG^{H_2O}, and C_m values were calculated from these kinetic data according to the method of Jackson and Fersht (23). The φ values were calculated as described by Chiti *et al.* (17).

Aggregation Kinetics—Aggregation of AcP and its variants was initiated by incubating the protein at a concentration of 0.4 mg/ml in 25% (v/v) TFE, 50 mM acetate buffer, pH 5.5, 25 °C. The kinetics of aggregates formation was monitored by mixing aliquots of 60 μl of the incubating solution with 440 μl of 25 mM phosphate buffer, pH 6.0, containing 25 μM ThT, at regular time intervals. Fluorescence measurements were carried out using a Shimadzu RF-5000 spectrofluorophotometer at excitation and emission wavelengths of 440 and 485 nm, respectively. The spectrofluorophotometer was thermostatted at 25 °C. Plots of ThT fluorescence against time were fitted to single exponential functions to determine the rate constants of aggregation.

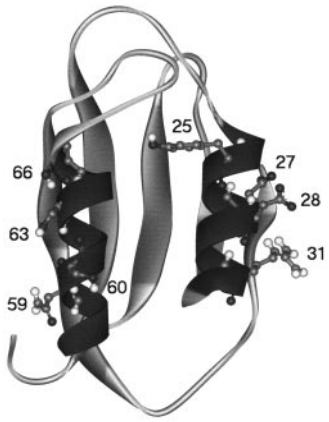

FIG. 1. **Schematic structure of AcP (36) drawn using the software WebLab Viewer, version 1.1.**

RESULTS

Choice of Mutations—Two α-helices are present in the native state of muscle AcP (Fig. 1), encompassing residues 22–32 (helix-1) and 55–67 (helix-2). Fig. 2 reports the α-helical propensity of the AcP sequence as determined by the AGADIR1 s-2 algorithm (24). The polypeptide sequence corresponding to helix-1 shows a remarkable α-helical propensity whereas that corresponding to helix-2 has virtually no inclination to form α-helical structure. Mutations aimed at changing the α-helical propensity of these two regions were designed using the AGADIR1 s-2 algorithm. Particular attention was paid to minimize the perturbation of the hydrophobic packing of the native state. For this reason only those residues completely exposed to the solvent and not involved in hydrophobic contacts were replaced.

The mutations chosen and their corresponding variants are as follows: Y25L/D28E, helix-1 (α+); E27N/D28N/R31N, helix-1 (α−/β+); E27T/D28T/R31T, helix-1 (α−/β+); and N59A/S60K/S63E/S66A, helix-2 (α+).

The effects of these substitutions on α-helical propensity are reported in Fig. 2. The stabilizing mutations of the helix-1 (α+) and helix-2 (α+) variants were selected to optimize electrostatic interactions and to increase the helical propensity of the inherent residues. Mutations involving a reduction of α-helical propensity of the region corresponding to helix-1 were chosen with an additional criterion, *i.e.* their effect on the propensity to form β-sheet structure. To this purpose, the scale of Street and Mayo (25) was used to evaluate whether the amino acid substitutions led to an increase or decrease of β-sheet propensity. Protein variants were generated in which, together with a destabilization of α-helical structure, the β-sheet propensity was minimized (helix-1, α−/β− mutant) and enhanced (helix-1, α−/β+ mutant), respectively.

Conformational Stability and Enzymatic Activity of Acylphosphatase Variants—The conformational stability of all AcP variants has been determined by means of equilibrium urea unfolding experiments at pH 5.5, 28 °C. Intrinsic fluorescence of pre-equilibrated samples has been measured in the presence of different urea concentrations, and the corresponding unfolding curves are reported in Fig. 3. Urea denaturation was found to be completely reversible under the experimental

[2] F. Chiti, N. Taddei, C. Capanni, N. Stefani, G. Rampoin, and C. M. Dobson, manuscript in preparation.

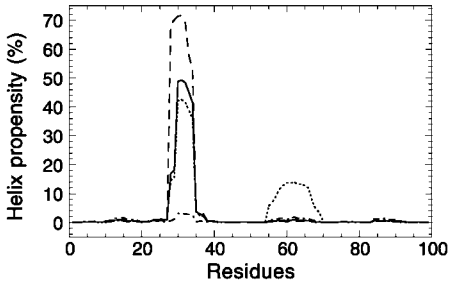

FIG. 2. **Plot of α-helical propensity (%) *versus* AcP sequence.** Wild-type AcP (*continuous line*), helix-1 (α+) (*dashed line*), helix-1 (α−/β−) (*dashed-dotted line*), helix-2 (α+) (*dotted line*). The calculation has been run using the software AGADIR1 s-2 (24) at www.embl-heidelberg.de/Services/serrano/agadir/agadir-start.html.

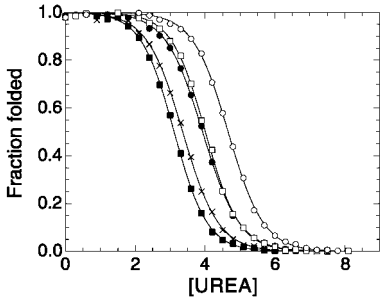

FIG. 3. **Equilibrium urea-induced denaturation of muscle AcP in 50 mM acetate buffer, pH 5.5, 28 °C.** Wild-type, *filled circle*; helix-1 (α+), *open square*; helix-1 (α−/β−), *filled square*; helix-1 (α−/β+), *crosses*; helix-2 (α+), *open circle*. The unfolding transition was monitored by following changes of intrinsic tryptophan fluorescence. Data are reported as the fraction of folded protein *versus* urea concentration. The fraction folded was calculated as $f_n = (y_d - y)/(y_d - y_n)$, where y is the fluorescence observed at a given urea concentration and y_d and y_n are the fluorescence signals of the denatured and native AcP, respectively, at the corresponding urea concentrations. The *solid lines* represent the fit of the data to the equation reported by Santoro and Bolen (22).

conditions used here. Table I summarizes the relevant thermodynamic parameters evaluated with the fitting procedure developed by Santoro and Bolen (22). The helix-2 (α+) variant results to be more resistant to urea denaturation and shows a significantly higher conformational stability, as indicated by the C_m and $\Delta G^{H_2O}_{U\text{-}F}$ values, respectively. The helix-1 (α+) variant possesses, within the experimental error, the same conformational stability of the wild-type protein. The introduction of mutations that decrease the helical propensity of the polypeptide chain (helix-1 (α−/β+) and helix-1 (α−/β−) variants) leads to moderate destabilization of AcP independently of the amino acid residue used for the replacement. The dependence of the free energy of unfolding on denaturant concentration, *i.e.* the m value, is very similar, within the experimental error, for all the species under investigation.

All protein variants display a significant enzymatic activity (Table I). It has been previously suggested that enzymatic activity can be used as a probe for the assessment of the native-like structure of an AcP protein variant, provided that the mutated residue does not participate to the catalytic mechanism and/or does not contribute to the formation of the active site (26). The activity measurements performed here clearly show that all these AcP variants maintain a native-like structural architecture. AcP active site is formed by residues belonging to the long 15–21 loop and a primary role in substrate binding is played by Arg-23, a residue positioned in the N-terminal region of helix-1 (27, 28). It can therefore be assumed that, during catalysis, this region undergoes those minor structural modifications required for an optimal catalytic efficiency. This necessarily implies a degree of flexibility of the active site region. The AcP variant carrying mutations that stabilize the helix-1 is the only one showing a significantly decreased enzymatic activity (Table I). The stabilization of the helix would increase the stiffness of the active site region giving rise to a non-optimized catalytic cycle, as it has been found to occur in the thermophilic counterparts of mesophilic enzymes. An alternative explanation for this fact is that the replacement of the residues Tyr-25 and Asp-28 in the helix-1 (α+) mutant determines a minor change of the geometry of the active site resulting in a decreased catalytic efficiency.

Kinetics of Folding—The rates of folding and unfolding were measured to understand the origin of the change of conformational stability. Stabilization or destabilization of a protein variant can arise from specific effects on either folding or unfolding rates or from a combination of effects on both rates. Refolding rates were measured following the intrinsic fluorescence changes upon dilution of urea-denatured AcP samples at different final urea concentrations. Unfolding kinetics were followed after placing fully native protein at different final denaturant concentrations. All kinetic traces were satisfactorily fitted to single-exponential functions. The natural logarithms of folding and unfolding rates as a function of denaturant concentration are reported in Fig. 4. Analysis of the data shown in the figure enabled us to evaluate the kinetic constants in water, $k_f^{H_2O}$ and $k_u^{H_2O}$, and the dependence of ln$k$ on urea concentration, m_f and m_u values. The absence of a downcurvature for refolding data points at low denaturant concentration, known as "roll-over," rules out that any of the protein variants used here fold with significant accumulation of intermediate species. Table II summarizes the relevant kinetic and thermodynamic parameters obtained from these measurements. The helix-2 (α+) AcP variant shows a remarkable increase (over 5-fold) of the refolding rate accompanied by a negligible effect on the unfolding rate. It is, therefore, straightforward to attribute the increased conformational stability of this variant to a specific increase of the rate of the folding reaction. The kinetic data permit the estimation of a ϕ value close to 1.0 for this AcP variant confirming the importance of the second α-helix in the folding process.

The helix-1 (α+) variant shows an increase, to comparable extents, of both folding and unfolding rates. This results in a basically unchanged conformational stability (Table II). Both helix-1 destabilized variants display a decrease of both folding and unfolding rates in water. From the kinetic constant values it is possible to determine the free energy change of the unfolding reaction that, for both mutants, was found not to be significantly different from that found for the wild-type protein (Table II). The conformational stability values calculated kinetically are in partial disagreement with the thermodynamic parameters obtained from equilibrium experiments (*cf.* Tables I and II) which indicate, at least in part, a destabilization of the two AcP variants. The discrepancy can be attributed to the different m values obtained from equilibrium and kinetic experiments for these variants. Indeed, the dependence of the unfolding rate on urea concentration, m_u, is significantly higher for the helix-1-destabilized variants as compared with the wild-type protein. A direct consequence of this fact is that the $k_u^{H_2O}$ values obtained by linear extrapolation are lower than the corresponding value of the wild-type protein, whereas, in the range of denaturing urea concentrations, the unfolding rates are always higher. The discrepancy between m values calculated from equilibrium and kinetic experiments has already been found for common-type AcP folding, and it cannot be simply attributed to uncertainties of measurements (29). A possible explanation for this observation is the presence of

TABLE I

Equilibrium urea-induced unfolding parameters and enzymatic activity of AcP variants

All experiments were performed at 28 °C, in 50 mM acetate buffer, pH 5.5 C_m is the urea concentration required to unfold 50% of the protein molecules. $\Delta G^{H_2O}_{U\text{-}F}$ is the Gibbs' free energy value of unfolding in the absence of urea, and m is the dependence of $\Delta G^{H_2O}_{U\text{-}F}$ on denaturant concentration. The enzymatic activity was measured using saturating concentrations of benzoylphosphate as a substrate, at pH 5.3 (21); one IU is defined as the enzymatic activity that hydrolyzes 1 μmol of substrate in 1 min at 25 °C. The average error for each m and $\Delta G^{H_2O}_{U\text{-}F}$ value is approximately 7%, for C_m is 0.15 M and for the enzymatic activity is 10%.

AcP variant	C_m	m	$\Delta G^{H_2O}_{U\text{-}F}$	Enzyme activity
	M	*kJ mol*$^{-1}$ *M*$^{-1}$	*kJ mol*$^{-1}$	*IU mg*$^{-1}$
Wild-type	3.93	4.76	18.69	3800
Helix-1 (α+)	4.01	5.16	20.68	1100
Helix-1 (α−/β−)	3.11	5.28	16.43	3400
Helix-1 (α−/β+)	3.36	4.90	16.48	3800
Helix-2 (α+)	4.66	4.94	23.03	2900

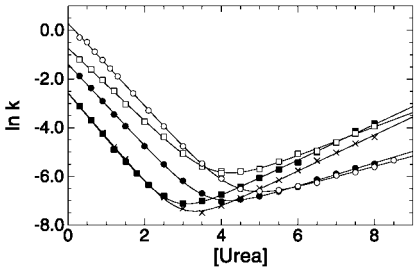

FIG. 4. **Natural logarithm of folding and unfolding rate constants of muscle AcP as a function of urea concentration.** All measurements were performed in 50 mM acetate buffer, pH 5.5, 28 °C. Wild-type, *filled circle*; helix-1 (α+), *open square*; helix-1 (α−/β−), *filled square*; helix-1 (α−/β+), *crosses*; helix-2 (α+), *open circle*. Data were fitted to the equation described by Jackson and Fersht (23).

native-like intermediates containing non-native *cis* X-Pro peptide bonds significantly populated at equilibrium (30).

The effects of the helix-1 mutations on the folding and unfolding rates are, in all cases, of similar nature. The helix-1 (α+) variant has both folding and unfolding rates increased; the two helix-1 (α−) variants have both the folding and unfolding rates decreased. These observations lead to estimates of ϕ values lower than 0 or higher than 1, which are attributable to the presence of non-native structure in the folding transition state. The change of the m_u value upon helix-1 mutation further complicates the attainment of reliable estimates of the ϕ value.

Aggregation Kinetics—Wild-type AcP undergoes aggregation in the presence of 25% (v/v) trifluoroethanol (TFE) at pH 5.5 (15). At the protein concentrations used here, TFE denatures the protein very rapidly, and aggregation develops from an ensemble of disordered conformations on a minute-hour time scale. Such protein aggregates convert subsequently to mature amyloid fibrils after a few weeks. It is possible to get a reproducible measure of the rate of formation of early aggregates by a simple optical test based on the binding of a fluorescent dye, thioflavin T, specific for amyloid[2]. Because the conformational stability of a protein is often of critical importance for the aggregation process (31–33), the experimental conditions used here cancel out the contribution of this factor and the measurement of the aggregation rate becomes a significant parameter accounting for the intrinsic propensity of AcP variants to aggregate.

Fig. 5 reports the kinetic traces of the aggregation process for all AcP variants. The fluorescence traces are satisfactorily fitted to single-exponential functions, and the aggregation rates derived from curve fitting are reported in Table III. Although the helix-2 (α+) variant shows an aggregation rate comparable to that of the wild-type protein, all variants carrying substitutions on helix-1 were found to aggregate with rates significantly different. Stabilization and destabilization of helix-1 causes the aggregation process to be decelerated and accelerated, respectively. In particular, the accelerating effect is much more marked for the variant carrying mutations that, in addition to decreasing the helical propensity, increase the propensity to form the β-structure. A 4-fold acceleration of aggregation is observed for the helix-1 (α−/β+) variant (Table III).

DISCUSSION

Implications for Protein Folding—Among the protein variants studied here, the only one showing a notable conformational stabilization, as demonstrated from equilibrium and kinetic folding experiments, is helix-2 (α+). All mutations within the helix-1 region of AcP lead to ΔG of global unfolding only marginally different from that of the wild-type protein, although the stability changes are those predicted on the basis of their effect on α-helical propensity. The ϕ value analysis of the kinetic data is a powerful method to assess the degree of consolidation of native-like contacts in the transition state for folding of those proteins whose refolding processes follow a two-state model (19). The ϕ value of nearly 1 for the helix-2 (α+) variant indicates that, in the transition state, helix-2 of AcP is consolidated to an extent similar to that in the native state. This finding is in agreement with previous results obtained for the highly homologous common-type AcP (7). For the reasons explained under "Results," the degree of formation of helix-1 in the transition state is difficult to evaluate. Some single point mutations of residues within helix-1 of AcP also led to ϕ values out of the 0–1 range, indicating the presence of non-native structure (17). Interestingly, molecular dynamics simulations provided a transition state structure with a non-native β-turn in the central portions of helix-1[3], an observation particularly intriguing when considering that such structural determination was not biased by the present experimental findings. The ability of helix-1 mutations to affect the unfolding rate indicates, however, that helix-1 is not fully formed in the transition state. Previous results obtained on the highly homologous common-type AcP indicate that helix-1 is 30–40% stabilized, compared with the native protein (7). Hence, the two helices of AcP play different roles in the folding process, helix-2 being more important to develop the folding transition state. Interestingly, both helix-1 and helix-2 have different α-helical propensities in the two isoforms. Helix-1 is more stable than helix-2 in muscle AcP. Nevertheless, when common-type AcP is considered, helix-2 is then the most stable one. Despite such differences, the extent of formation of each of the two helices in the transition state is comparable in the two isoenzymes, reinforcing the theory that overall topology, as opposed to local conformational preferences, determine a key role in the folding mechanism of proteins displaying the topology of AcP (17).

Aggregation versus Folding—The effects of various mutations studied here on the rate of folding are very different from

[3] E. Paci, personal communication.

TABLE II
Relevant kinetic and thermodynamic parameters

All the experiments were performed in 50 mM acetate buffer, pH 5.5, at 28 °C. Experimental errors, given by the fitting procedure, are as follows: $k_f^{H_2O}$ and $k_u^{H_2O}$, 10%; m_f and m_u, 5%; C_m, 0.3 M; m and $\Delta G_{U\text{-}F}^{H_2O}$, 5%.

AcP variant	$k_f^{H_2O}$	$k_u^{H_2O}$	m_f	m_u	m	C_m	$\Delta G_{U\text{-}F}^{H_2O}$
	s^{-1a}			M^{-1a}	$kJ\ mol^{-1}\ M^{-1b}$	M^b	kJ/mol^b
Wild-type	0.25	0.96×10^{-4}	1.69	0.48	5.43	3.62	19.68
Helix-1 (α+)	0.49	1.66×10^{-4}	1.51	0.59	5.26	3.80	19.99
Helix-1 (α−/β−)	0.076	0.59×10^{-4}	1.87	0.73	6.50	2.76	17.93
Helix-1 (α−/β+)	0.077	0.36×10^{-4}	1.84	0.74	6.46	2.97	19.19
Helix-2 (α+)	1.34	1.25×10^{-4}	1.70	0.42	5.31	4.37	23.22

[a] Parameters obtained by fitting of the data reported in Fig. 4.
[b] Parameters obtained according to Jackson and Fersht (23).

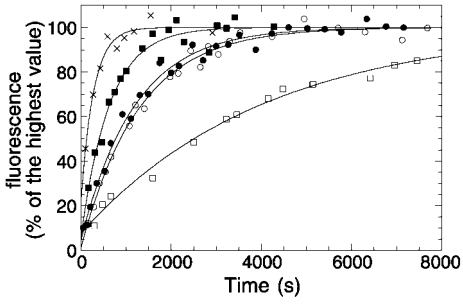

FIG. 5. **Aggregation kinetics of AcP variants in 50 mm acetate buffer, pH 5.5, 28 °C, in the presence of 25% (v/v) TFE.** Wild-type, *filled circle*; helix-1 (α+), *open square*; helix-1 (α−/β−), *filled square*; helix-1 (α−/β+), *crosses*; helix-2 (α+), *open circle*. Data are reported as the percentage of the maximum ThT fluorescence value as a function of time. Each curve was fitted to a single-exponential function (*solid lines*).

TABLE III
Aggregation rates of AcP variants

AcP variant	k_{aggr}	$k'_{aggr}/k_{aggr}{}^b$	$k'_f/k_f{}^b$
	s^{-1a}		
Wild-type	9.4×10^{-4}	1	1
Helix-1 (α+)	2.4×10^{-4}	0.26	1.96
Helix-1 (α−/β−)	15.7×10^{-4}	1.67	0.30
Helix-1 (α−/β+)	39.0×10^{-4}	4.15	0.31
Helix-2 (α+)	7.8×10^{-4}	0.83	5.36

[a] Aggregation experiments were performed at 25 °C, in 50 mM acetate buffer, pH 5.5, in the presence of 25% TFE (v/v). The average error for k_{aggr} is 10%.
[b] k'_{aggr} and k_{aggr} are the aggregation rates of the variant and wild-type protein, respectively. k'_f and k_f are the folding rates in water of the variant and wild-type protein, respectively.

those observed on the rate of aggregation (Table III). The replacements on helix-2, although causing the folding rate to be considerably accelerated, do not affect the aggregation rate significantly. A recent and systematic mutational analysis has shown that, in the aggregation process of AcP taking place from a partially denatured ensemble, a region, including helix-1, plays a crucial role whereas helix-2 is not relevant.[2] The inability of the mutations stabilizing helix-2 to affect the aggregation rate is consistent with this region being non-critical in the aggregation process. By contrast, the change of aggregation rate upon mutation within helix-1 is consistent with the crucial role played by such a region in aggregation. Such changes are, however, opposite to those observed on folding rate. From the values reported in Table III, it is clear that destabilization of helix-1 decelerates folding and accelerates aggregation and that the opposite effects are caused by stabilization of the helix. The two sets of mutations destabilizing helix-1 produce similar effects on folding and favor aggregation to different extents as a result of the different contribution of these mutations on β-sheet propensity. When environmental conditions, such as those used in our experiments to promote aggregation, disfavor thermodynamically normal folding, the secondary structure-forming propensities of the polypeptide chain become critical factors in determining the aggregation efficiency. Both α and β propensity appear to be relevant. Only α-helical propensity appears, on the other hand, critical for folding, most likely because the mutated region is committed to this type of secondary structure in the native state.

The results obtained using AcP as a model system are in very good agreement with a recent study, in which the relationships between theoretical secondary structure predictions and the actual structure of the native state have been investigated for a number of amyloid-forming proteins (34). Some of these pathologic proteins, such as the prion protein, the Alzheimer's amyloid β-peptide, and the lung surfactant protein C, contain discordant helices, *i.e.* secondary structural elements that are helical in the native structure but, according to the theoretical predictions, display a very poor α-helical propensity and a high inclination to form β-structure. When residues placed within these helices are substituted to increase the helical propensity of the polypeptide chain, the resulting protein variants do not undergo aggregation and fibril formation (34). Similar results have also been obtained for the activation domain of human procarboxypeptidase (35). Protein variants carrying mutations aimed at increasing the local stability of the helical regions of the native state reduce the aggregation propensity of this protein (35).

Conclusions—A kinetic partitioning of folding and aggregation exists as the two α-helical regions characterizing the native state of AcP have distinct relevance in the two processes. This partitioning does not reflect the difference in intrinsic α-helical propensities of the two helices, indicating that both processes of folding and aggregation are specific and do not initiate from regions that have simply secondary structure propensities favorable for such processes. Despite this, folding and aggregation are both sensitive to changes of α-helical propensity of the relevant regions. Mutations enhancing the α-helical propensity increase the rate of folding and decrease that of aggregation as long as the mutated helices are at least partially formed in the transition state for folding and involved in the rate-determining steps of aggregation, respectively. In addition to underlying the fundamentals of folding and aggregation, these findings are also relevant for understanding how protein sequences have evolved and for providing simple rules in protein design. An evolutionary pressure must have existed not just to favor folding to specific globular structures but also to render aggregation less competitive than folding. Identification of the regions involved in the aggregation process and design of their sequence with a relatively high α-helical propensity and a low tendency to form β-sheet structure may aid significantly the attainment and maintenance of stable folding.

REFERENCES

1. Goldenberg, D. P. (1999) *Nat. Struct. Biol.* **6,** 987–990
2. Ionescu, R. M., and Matthews, C. R. (1999) *Nat. Struct. Biol.* **6,** 304–307
3. Baldwin, R. L., and Rose, G. D. (1999) *Trends Biochem. Sci.* **24,** 26–33
4. Muñoz, V., Cronet, P., López Hernández, E., and Serrano, L. (1996) *Folding*

Des. **1,** 167–178
5. Viguera, A. R., Villegas, V., Aviles, F. X., and Serrano, L. (1997) *Folding Des.* **2,** 23–33
6. Zitzewitz, J. A., Ibarra-Molero, B., Fishel, D. R., Terry, K. L., and Matthews, C. R. (2000) *J. Mol. Biol.* **296,** 1105–1116
7. Taddei, N., Chiti, F., Fiaschi, T., Bucciantini, M., Capanni, C., Stefani, M., Serrano, L., Dobson, C. M., and Ramponi, G. (2000) *J. Mol. Biol.* **300,** 633–647
8. Martinez, J. C., and Serrano, L. (1999) *Nat. Struct. Biol.* **6,** 1010–1016
9. Mok, Y.-K., Elisseeva, E. L., Davidson, A. R., and Forman-Kay, J. D. (2001) *J. Mol. Biol.* **307,** 913–928
10. Bellotti, V., Mangione, P., and Stoppini, M. (1999) *Cell. Mol. Life Sci.* **55,** 977–991
11. Kelly, J. W. (1998) *Curr. Opin. Struct. Biol.* **8,** 101–106
12. Sunde, M., and Blake, C. C. F. (1997) *Adv. Protein Chem.* **50,** 123–159
13. Dobson, C. M. (1999) *Trends Biochem. Sci.* **9,** 329–332
14. van Nuland, N. A. J., Chiti, F., Taddei, N., Raugei, G., Ramponi, G., and Dobson, C. M. (1998) *J. Mol. Biol.* **283,** 883–891
15. Chiti, F., Webster, P., Taddei, N., Stefani, M., Ramponi, G., and Dobson, C. M. (1999) *Proc. Natl. Acad. Sci. U. S. A.* **96,** 3590–3594
16. Chiti, F., Taddei, N., van Nuland, N. A. J., Magherini, F., Stefani, M., Ramponi, G., and Dobson, C. M. (1998) *J. Mol. Biol.* **283,** 893–903
17. Chiti, F., Taddei, N., White, P. M., Bucciantini, M., Magherini, F., Stefani, M., and Dobson, C. M. (1999) *Nat. Struct. Biol.* **6,** 1005–1009
18. Vendruscolo, M., Paci, E., Dobson, C. M., and Karplus, M. (2001) *Nature* **409,** 641–645
19. Fersht, A. R. (1999) *Structure and Mechanism in Protein Science: A Guide to Enzyme Catalysis and Protein Folding*, pp. 558–563, W. H. Freeman and Co., New York, NY
20. Taddei, N., Stefani, M., Magherini, F., Chiti, F., Modesti, A., Raugei, G., and Ramponi, G. (1996) *Biochemistry* **35,** 7077–7083
21. Ramponi, G., Treves, C., and Guerritore, A. (1966) *Arch. Biochem. Biophys.* **115,** 129–135
22. Santoro, M. M., and Bolen, D. W. (1988) *Biochemistry* **27,** 8063–8068
23. Jackson, S. E., and Fersht, A. R. (1991) *Biochemistry* **30,** 10428–10435
24. Lacroix, E., Viguera, A. R., and Serrano, L. (1998) *J. Mol. Biol.* **284,** 173–191
25. Street, A. G., and Mayo, S. L. (1999) *Proc. Natl. Acad. Sci. U. S. A.* **96,** 9074–9076
26. Paoli, P., Taddei, N., Fiaschi, T., Veggi, D., Camici, G., Manao, G., Raugei, G., Chiti, F., and Ramponi, G. (1999) *Arch. Biochem. Biophys.* **363,** 349–355
27. Taddei, N., Stefani, M., Vecchi, M., Modesti, A., Raugei, G., Bucciantini, M., Magherini, F., and Ramponi, G. (1994) *Biochim. Biophys. Acta* **1208,** 75–80
28. Taddei, N., Chiti, F., Magherini, F., Stefani, M., Thunnissen, M. M. G. M., Nordlund, P., and Ramponi, G. (1997) *Biochemistry* **36,** 7217–7224
29. Taddei, N., Chiti, F., Paoli, P., Fiaschi, T., Bucciantini, M., Stefani, M., Dobson, C. M., and Ramponi, G. (1999) *Biochemistry* **38,** 2135–2142
30. Chiti, F., Taddei, N., Giannoni, E., van Nuland, N. A. J., Ramponi, G., and Dobson, C. M. (1999) *J. Biol. Chem.* **274,** 20151–20158
31. Hurle, M. R., Helms, L. R., Li, L., Chan, W., and Wetzel, R. (1994) *Proc. Natl. Acad. Sci. U. S. A.* **91,** 5446–5450
32. Booth, D. R., Sunde, M., Bellotti, V., Robinson, C. V., Hutchinson, W. L., Fraser, P. E., Hawkins, P. N., Dobson, C. M., Radford, S. E., Blake, C. C. F., and Pepys, M. B. (1997) *Nature* **385,** 787–793
33. Chiti, F., Taddei, N., Bucciantini, M., White, P., Ramponi, G., and Dobson, C. M. (2000) *EMBO J.* **19,** 1441–1449
34. Kallberg, Y., Gustafson, M., Persson, B., Thyberg, J., and Johansson, J. (2001) *J. Biol. Chem.* **276,** 12945–12950
35. Villegas, V., Zurdo, J., Filimonov, V. V., Aviles, F. X., Dobson, C. M., and Serrano, L. (2000) *Protein Sci.* **9,** 1700–1708
36. Thunnissen, M. M. G. M., Taddei, N., Liguri, G., Ramponi, G., and Nordlund, P. (1997) *Structure* **5,** 69–79

Folding and Aggregation Are Selectively Influenced by the Conformational Preferences of the α-Helices of Muscle Acylphosphatase

Niccolò Taddei, Cristina Capanni, Fabrizio Chiti, Massimo Stefani, Christopher M. Dobson and Giampietro Ramponi

J. Biol. Chem. 2001, 276:37149-37154.
doi: 10.1074/jbc.M105720200 originally published online July 30, 2001
